Spring 2010

A numerical investigation of flowfield modification in high-speed airbreathing inlets using energy deposition

Matthew Flynn Rohweder

Department:

A NUMERICAL INVESTIGATION OF FLOWFIELD MODIFICATION IN HIGH-SPEED AIRBREATHING INLETS USING ENERGY DEPOSITION

by

MATTHEW FLYNN ROHWEDER

A THESIS

Presented to the Faculty of the Graduate School of the

MISSOURI UNIVERSITY OF SCIENCE AND TECHNOLOGY

In Partial Fulfillment of the Requirements for the Degree

MASTER OF SCIENCE IN AEROSPACE ENGINEERING

2010

Approved by

David W. Riggins, Advisor
Kakkattukuzhy M. Isaac
Joshua L. Rovey

ABSTRACT

Energy deposition in front of dual-mode ram/scramjet engines is numerically investigated utilizing two-dimensional CFD for its potential to modify inlet/isolator flow-fields for engine start/unstart control and for its general potential for generating large-scale flow-field modification in such flows. A simplified (high Mach number) constant-area duct geometry is initially defined in order to test the feasibility of the concept; the results from this initial investigation demonstrates possible beneficial effects of depositing energy upstream of a thermally choked duct in terms of causing massive changes in flow patterns, including the reestablishment of supersonic flow throughout the duct. This study is followed by the definition of a realistic high-speed engine domain focusing on the lower external and internal engine side of a hypersonic vehicle. A quasi-one-dimensional solver is constructed and used to establish approximate understanding of thermal choking limits in the defined geometry. A CFD investigation of this actual engine geometry is performed in which heating blocks are used to simulate fuel-air combustion in the engine combustor. Actual choking limits are established and a base-line case defined with substantial (choked flow) upstream interaction. A range of energy deposition cases are then run in order to assess the use of upstream energy deposition for facilititating restarting an unstarted engine, mitigating unstart, and generating large-scale flow-field modification in the isolator/inlet of a dual-mode ram/scramjet engine. Results indicate that, although the ability to actually increase performance of an unstarted engine through the use of upstream energy deposition is minimal, there is indication that the use of such a technique for generating a ‘virtual cowl’ and/or a ‘virtual’ isolator (including throats, etc.) is possible.

ACKNOWLEDGMENTS

This author would like to thank Dr. David Riggins for his assistance throughout both this work and this author's entire collegiate experience. His guidance during this author's undergraduate and graduate experience as well as throughout this author's military career have been instrumental. This author would also like to thank the other members of the committee, Dr. Kakkattukuzhy M. Isaac and Dr. Joshua L. Rovey, for their contributions to this work.

This author would like to thank Christopher Marley for his work on the initial "proof-of-concept" analysis as well as his assistance with GridGen and VULCAN CFD software.

This author would also like to thank the AFOSR summer researcher program at Wright-Patterson Air Force Base for their support.

Lastly, this author would like to thank his parents, Michael and Laurie Rohweder, for their continual support over the years. And this author would also like to thank his brother, LCpl Seth Michael Rohweder, USMC, for helping him to remain grounded throughout this author's varied and occasionally foolhardy endeavors.

TABLE OF CONTENTS

LIST OF ILLUSTRATIONS

Page

LIST OF TABLES

Page

NOMENCLATURE

Symbol	Description
A_{min}	Minimum cross-sectional area (m^2)
A_o	Upstream capture area (m^2)
Mo	Freestream Mach number
γ	Ratio of specific heats
ρ	Density (kg/m^3)
$\vec{V}$	Velocity vector (m/s)
$\hat{n}$	Unit normal vector
dS	Differential surface area (m^2)
S	Surface area (m^2)
P	Pressure (Pa)
τ_w	Shear stress (Pa)
c	Circumference (m)
dx	Differential length (m)
e	Specific internal energy (J/kg)
u	Velocity component in axial direction (m/s)
$\delta\dot{Q}$	Rate of heat transfer to system (W)
A	Area (m^2)
h	Specific enthalpy (J/kg)
T	Temperature (K)
R	Gas constant (J/kg-K)
α_l	Species mass fraction
C_p	Specific heat at constant pressure (J/kg-K)
$\dot{m}$	Mass flow rate (kg/s)
F	Force (N)
F_x	Force in local axial direction (N)

1. INTRODUCTION

The use of focused energy deposition in hypersonic flows for achieving a number of potentially beneficial effects has been well documented, both numerically and experimentally. Applications for energy deposition include shock wave modification in front of blunt bodies for large-scale drag reductions and for generating control forces and moments on aerodynamic surfaces. An application strongly related to the present study is the use of targeted energy deposition in order to deflect the flow upstream of air-breathing scramjet engine inlets such that mass flow rate of air inducted into the engine is increased. The current investigation is specifically focused on analyzing the potential use of energy deposition for 1) maintaining 'started' high-speed dual mode ram/scramjet engine flow, 2) recovering or increasing operability of such an engine which has 'unstarted' (i.e. allowing recovery or some mitigation from a condition of complete unstart), and 3) generating large-scale flow-field modification using energy deposited upstream of unstarted/started dual-mode ram/scramjet engines. In this work, unstart is defined as the condition in which the engine has disgorged a shock and is essentially operating in a largely subsonic mode, or more precisely as the condition in which a high speed engine has a vertical plane of subsonic flow extending from the leading edge of the cowl (inlet) up to the body with accompanying large-scale (subsonic) mass spillage. Conversely, a 'started' high-speed engine has fully supersonic flow (except for thin or moderate boundary layers along walls) entering the internal ducting of the engine. These definitions are somewhat different than those used by Bao, Chang, Yu, and Xie [1] for

started and unstarted flow; they define unstart as the presence of separated flow and shocks at the inlet face, without explicitly mentioning spillage of mass.

The prevailing strategy for operation of a high-speed scramjet (dual mode ram/scramjet or pure scramjet) engine has been to simply avoid operating at flight and configurational conditions which could lead to unstart, due to the large losses in both total pressure through upstream shock structures and mass capture which result when the engine is unstarted. This has placed obvious limits on the operability envelopes and flight regimes for dual-mode ram/scramjet and scramjet systems. The ability to mitigate unstart (lessen its detrimental effects), or even recover from unstart, by utilizing relatively small amounts of energy in targeted zones in the upstream/adjacent flow could prove beneficial in terms of expanding the envelope of engine performance and increasing the robustness (operability) of the engine at off-design conditions.

While there have been a variety of studies on the use of energy deposition for a myriad of flowfield modification applications, no known studies have analyzed the potential impact of energy deposition for mitigating and/or recovering from engine unstart in a hypersonic inlet or the general impact of energy deposition on such flows; this study is believed to represent the first attempt at analyzing such an application. In addition, as a part of the current effort, the potential of using energy deposition upstream of the internal engine flow-field in order to create a 'virtual cowl' (for instance to control engine contraction ratio or entering flow characteristics using flow-field modification rather than a physical surface forward of the internal engine) will also be examined.

The central objective of the current investigation is therefore to perform a numerical study of the use of energy deposition in the inlet flow-field (generally locating

the energy deposition upstream of the internal engine ducting) for delaying unstart and for the possible mitigation of unstart and possible recovery from unstart. In addition, other possible operability/performance benefits of energy deposition in dual-mode ram/scramjet engine flow-fields, including the 'virtual cowl' concept will be examined.

In terms of engine unstart control, energy deposition could (conceptually) allow a dynamic and non-structural control for unstart (or incipient unstart) phenomena and possibly increase ranges of fueling amounts and reduce or even eliminate the need for the isolator component. The isolator component, which is a key component of a dual mode ram/scramjet engine (as will be discussed in a subsequent section) is heavy and significantly increases the length and hence losses associated with the engine. Note that current techniques for recovering from unstart would include the technique of either changing the flight/operating point of the vehicle appropriately (i.e. overspeed the engine) or mechanically changing the engine geometry.

In addition to the application of energy deposition for unstart control in an engine, of interest in the current investigation is the use of energy deposition to effect large scale changes in flow-field character upstream and in the inlet/isolator of a ram/scramjet engine system. While the use of a 'virtual cowl' concept utilizing energy deposition for improving engine mass capture has been examined in previous work (see Literature Review section), the opposite effect, in which the effective internal inlet face capture area can be adjusted (i.e. reduced) to in order to increase the overall forebody/inlet contraction ratio, needs examination as well. This could be (possibly) beneficial in terms of maintaining or controlling engine performance for varying flight Mach numbers of the vehicle. Specifically, energy deposition could conceptually be used for more dynamic

control of the inflow conditions without the added external structure (although the additional mass associated with energy deposition systems would necessarily increase vehicle weight and entail system issues which are not investigated here). For example, energy deposition may allow the inlet to be physically sized for high-speed scramjet operation (or conversely for 'low-speed' ramjet operation) but, through the use of a virtual cowl and/or a virtual (i.e. non-physical) converging diffuser/isolator via energy deposition, performance could possibly be maintained across the Mach number range, as well as allowing/facilitating starting or controlling the flow and transitioning from ramjet to scramjet operation. This approach can conceptually be clarified by examining the familiar isentropic area-Mach relationship for fluid in a streamtube:

$$\left(\frac{A_{min}}{A_o}\right) = M_o * \left(\frac{\gamma+1}{2}\right)^{\frac{\gamma+1}{2*(\gamma-1)}} * \left(1+\frac{\gamma-1}{2}M_o^2\right)^{\frac{-\gamma-1}{2*(\gamma-1)}} \quad (1)$$

In this equation, A_{min} is the minimum cross-sectional area (corresponding to the inlet physical throat for a ramjet engine), A_o is the upstream capture area, γ is the ratio of specific heats, and M_o is the freestream Mach number. As can be seen from this relationship, as the freestream Mach increases, the ratio of throat area required to choke the flow to capture area decreases (i.e. the required contraction ratio for the engine increases). Energy deposition could (conceptually) be used to deflect and channel a flow entering an engine and control contraction ratio non-mechanically and even create (and control) an artificial (choked) throat.

The organization of this thesis is as follows: Section 2 provides a literature review in which previous work on both energy deposition applications and dual mode

ram/scramjet engine studies is summarized, along with a discussion of the very limited work done on the use of energy deposition in dual mode ram/scramjet engine flow-fields. Section 3 discusses the physics of a dual mode ram/scramjet with emphasis on the isolator component and associated flow-fields and on the phenomena of engine unstart. This is followed by Section 4 which is a brief review of a preliminary ('proof-of-concept') investigation using energy deposition for mitigating unstart-like phenomena utilizing a highly simplified 'engine-like' geometry. Section 5 discusses the main geometry analyzed in this work (corresponding to the forebody/engine/aftbody section of a representative hypersonic vehicle) while Section 6 reviews the CFD code and methodology. Section 7 provides an analytical investigation of choking limits in the defined geometry, using a quasi-one-dimensional solver developed for this investigation. Section 8 focuses on the numerical results obtained in this study and Section 9 describes temporal and grid convergence studies for the present simulations. Finally, Section 10 provides a summary of the major results of the current investigation along with an overview of recommended future work on this topic.

2. HISTORY AND LITERATURE REVIEW

This section provides a discussion of some of the relevant previous work done on the applications of energy deposition in high-speed flow-fields. This is done in order to provide context and background for the objective and methodology of the current study.

The use of energy deposition in high-speed flows for flow-field modification is not a new concept and has previously been shown to be potentially useful in a number of previous studies, both numerical and experimental. Several studies using energy deposition for drag reduction have shown promise, including those by Riggins et al. ([2] and [3]). Work done by Riggins, Nelson and Johnson [4] have shown that energy deposited in the freestream upstream of a blunt body in hypersonic flow caused a 45-70% reduction in drag (i.e. drag of body with upstream energy deposition normalized to drag with no upstream energy deposition). This work detailed a numerical investigation of comparative drag reductions utilizing upstream energy deposition with the drag reduction obtained on the same blunt body utilizing an installed (physical) spike. Results for 2-D blunt body at flight Mach 6.5 showed decreasing drag with increasing upstream energy amount. The drag reduction (per meter width) asymptotically approached 45% to 50%, depending on the amount of energy deposited upstream of the blunt body. In this same study, similar (but more pronounced) results were obtained in this investigation for an axisymmetric blunt body geometry at a flight Mach number of 10. This study resulted in drag reductions ranging from 25% to a dramatic 70%, depending on the energy deposition location upstream of the blunt body. Other work using energy deposition was performed by Bisek, Boyd, and Poggie [5]. This work studied the use of energy

deposition for the aerodynamic control of hypersonic vehicles; results were compared to the use of conventional mechanical controls. Using Mach 12 flow and freestream condition at 40 km altitude, these researchers evaluated the impact of using three different deposition geometries for flight control: a spherical region of energy deposition, an oblate spheroid region of energy deposition (referred to as a pancake), and a prolate spheroid region of energy deposition (referred to as a bean). A range of 1-15 kW was used for deposition near the forward end of a three-dimensional blunt elliptical cone. Location of deposition was near the leading edge bow shock in order to maximize moment arm and maximal force changes (as determined by Menart et al. [6]). The final results of this analysis was that the same order of magnitude of control could be achieved with the energy deposition as with a mechanical flap based on comparing moment coefficients. They also noted that the moment coefficient generated with energy deposition was independent of the geometry of energy deposition. While there were differences in the local pressure coefficients, the geometry of the deposition zone had no impact on moments for aerodynamic control. This independence on deposition geometry will be further evaluated in the course of this study, as applied to the engine unstart phenomena.

Shneider, Macheret, Zaidi, Girgis and Miles [7] at Princeton used energy deposition (with energy amounts used ranging from 2-3.5% of inlet enthalpy flow rate) located just forward and below the cowl leading edge in a hypersonic inlet in order to improve mass capture (into the engine). They reported mass capture increases of between 15-20%. The geometry used in this analysis was a three-ramp inlet designed so that a Mach 10 freestream flow would just miss the cowl lip at zero angle of attack.

Cases of freestream Mach numbers of Mach 6, Mach 8, and Mach 10 with dynamic pressure of 1000 pounds per square foot (psf) and 2000 psf were evaluated. The location of the energy deposition was initially chosen at the intersection of the leading edge shock with the leading edge extension of the cowl. However, in order to avoid ingesting any of the heated flow the location was shifted to just below the cowl leading edge. Up to 10 megawatts (MW) was deposited upstream. At a freestream Mach of 6, this 10 MW corresponded to 3.4% of the enthalpy flux into the inlet and resulted in an increase of mass capture of up to 20%. It should also be noted that results from this study indicate that as the Mach was lowered from 10 to 6, higher and higher upstream energy deposition amounts as a percentage of inlet enthalpy flux were necessary in order to show the same improvements in mass flow rate.

These results led to further investigation into what has been labeled the "virtual cowl" concept. Typically, an inlet is designed for the maximum flight Mach number it is intended to experience and its geometry is designed such that it will obtain shock-on-lip condition (oblique shock emanating from the body leading edge terminating at (or more practically just missing) the leading edge of the cowl). When not operating at this shock-on-lip condition, subsequent mass-spillage will occur (in which some portion of the air which has been compressed by the forebody shock(s) does not enter the entrance to the internal inlet of the engine, i.e. sweeps under the cowl leading edge and below the vehicle). As noted in the work by Macheret, et al., the use of upstream energy deposition can be used to increase mass capture and limit spillage.

3. BACKGROUND – DISCUSSION OF UNSTART MECHANISMS AND FLOW PHYSICS – ISOLATOR PHYSICS

This section provides a discussion of the flow physics in a dual mode ram/scramjet engine with emphasis on isolator behavior and unstart. Scramjet engine operation above a flight Mach number of around 7 or 8 is characterized by predominantly supersonic flow throughout the combustor. Areas of recirculation are generally small and are mainly confined to the aft surfaces of intrusive fuel injectors or associated with very local regions around flush-wall jets or rearward-facing surfaces. There is little upstream interaction in such a flow; limited interaction may occur due to information propagation upstream through relatively thin wall boundary layers, but this limited interaction does not affect the bulk upstream flow in any significant fashion. The critical ratio of heating rate caused by fuel-air combustion in the burner to entering total enthalpy rate is very small. This fact results in low pressure rises in the downstream burner (even with modest cross-sectional area increases) with the result that large-scale sub-sonic regions (or regions of separated flow) are not established. The combustor entrance conditions are then essentially de-coupled from the flow-field within the combustor. Furthermore, the degree of diffusion throughout the inlet/combustor system is not sufficient to cause the flow Mach number (even within the combustor) to approach unity, hence the issue of choking and engine unstart is generally avoided. For the high-speed range, then, there is little ambiguity (although considerable challenge) for the engineer, at least in terms of understanding the broad design issues, requirements, and dominant flow features for the scramjet (in terms of predicting and analyzing performance and operability). A depiction of this geometry and flowfield can be seen in Fig. 3.1 below.

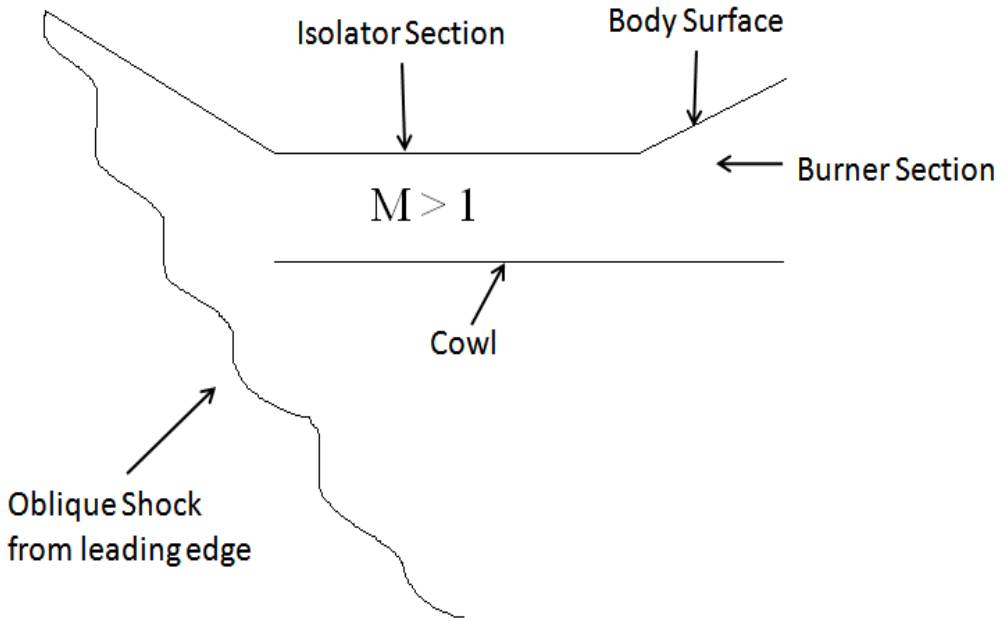

Figure 3.1. Example of started flow for a representative hypersonic geometry

As flight Mach number is lowered below Mach 7 for a scramjet engine, some significant effects drastically change flow character, engine performance, and engine operability. The ratio of heating rate (due to fuel-air combustion) to entering total enthalpy rate becomes large. Significant pressure rise is experienced in the combustor. This pressure rise due to heat release is coupled with the decrease of the Mach number in the combustor so that Mach 1 can result. Eventually, the flow is back-pressured enough such that significant interaction occurs upstream of the fuel injection location/combustor entrance; this interaction develops as an upstream oblique shock train with associated large recirculation (or low velocity) regions adjacent to walls (see Fig. 3.2 below). A high-speed scramjet operated at such conditions (‘mid-speed’ flight Mach numbers) will have this phenomena immediately propagate into the inlet. Due to the difficulties and

inherent instability associated with maintaining this shock system in a converging flowpath, inlet/engine unstart may result. For this reason, the component known as an isolator is generally incorporated between inlet and combustor for mid-speed scramjets – this component buffers the inlet from upstream propagating interaction from the combustor. The oblique shock system and associated pattern of recirculation regions will stabilize in the isolator such that started engine operation is maintained, even with extensive upstream interaction (provided the isolator is long enough). Several other techniques can also be used including 1) backward facing steps at the entrance of the combustor proper or at various locations along the combustor (these tend to isolate or stabilize recirculation and slow the development of extensive upstream interactions), 2) diverging combustor walls in order to relieve the combustion-generated pressure rise, delay the development of a possible thermal choke, and facilitate reestablishment of supersonic flow subsequent to thermal choking and 3) axially staged injection which can 'distribute' heat release appropriate to combustor geometry and varying inflow conditions.

The variance of flow features observed for the scramjet combustor operated at mid-speed conditions is therefore astonishingly large. As examples: bulk flow may or may not remain supersonic, thermal choking may or may not occur, upstream recirculation bubbles may extend far downstream into the combustor proper (in fact, some rig-specific experimental data indicates recirculation blanketing the entire combustor), localized oblique and normal shocks can truncate the oblique shock train in the isolator or at the combustor entrance, and the isolator flow can form an effective (distortion-induced) aerodynamic throat. Such flows are highly complex, strongly

coupled, massively elliptical in character, contain complex turbulence mechanisms and physics; they represent an extreme challenge for analysis, numerical simulation, or experimental work.

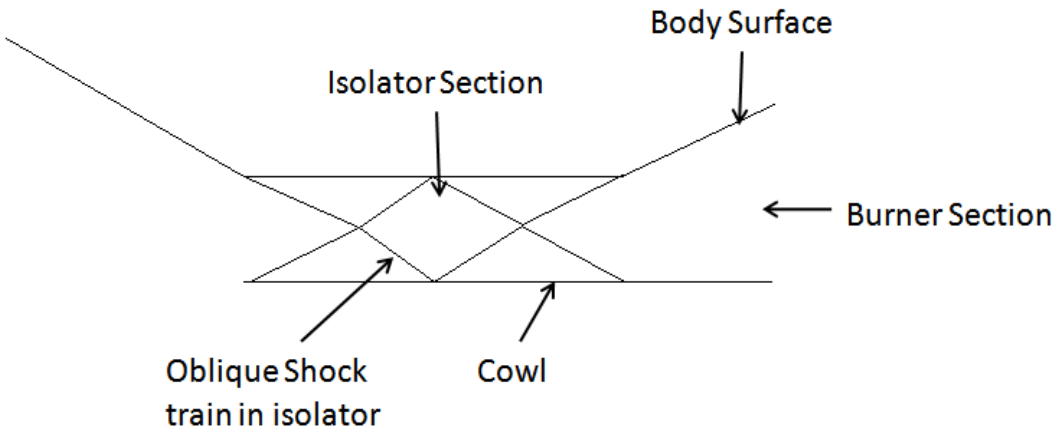

Figure 3.2. Oblique shock train in isolator section

Note that, for a started flow, a variety of mechanisms or effects can lead to unstart. First, for a started inlet, if the incoming Mach number is reduced below the starting value Mach number for the fixed-area inlet contraction ratio, the engine can disgorge a shock upstream of the inlet. Another cause of unstart can be large and/or transitory changes to the incoming flow. These changes could be the result of changes to the angle of attack leading to a physical blockage, a build-up of the boundary layer causing boundary layer blockage, or even a change in the chemical composition of the freestream air. Another mechanism for inducing or causing unstart is related to engine

backpressure effects, generally occurring due to heat addition in the combustor component (also known as a burner) This mechanism of heat release-induced unstart and inlet forcing will be of interest in this investigation. A visual representation of unstart can be seen in Fig. 3.3.

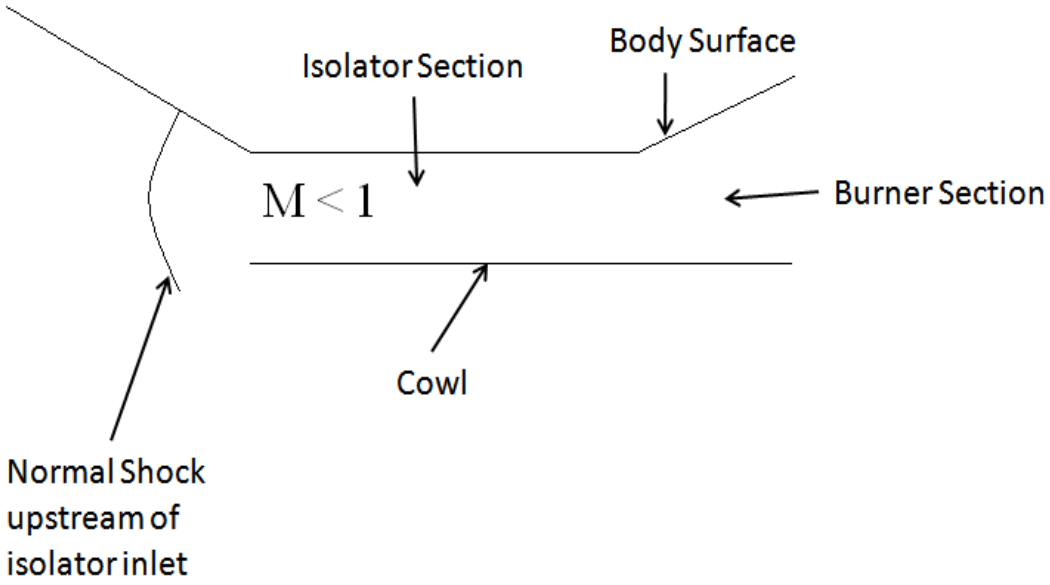

Figure 3.3. Unstarted flow with normal shock upstream of isolator inlet

The transient nature of the fluid dynamics associated with the unstart condition is important as well although it is often not discussed in the literature. Work by Guo and Tan [8] investigated the development of unstart in a started inlet and subsequent self-start. Data were experimentally determined by controlling backpressure via a variable plug at the aft end of a constant area duct. The inlet was designed for a shock-on-lip condition at a freestream Mach number of 6 and a contraction ratio of 7. 0% denotes no

flow blockage using the plug and 100% represents complete blockage at the aft end of the duct. The percent blockage was varied from 0% to 100% while observing unsteady transients in the flow. At 89% blockage, the back pressure from the mass accumulation in the duct was finally sufficient to disgorge the shock system from the inlet. This transient condition from started flow to unstart caused a flow reversal inside the duct prior to subsequent re-ingestion of the shock system and restarting of the inlet. Besides the large pressure transients experienced, this flow reversal could also introduce hot gas from the products of combustion into the inlet where there is likely to be less thermal protection.

4. PRELIMINARY ENERGY DEPOSITION 'PROOF-OF-CONCEPT' CONFIGURATION

An initial 'proof-of-concept' investigation of the utilization of energy deposition was performed in order to ascertain whether potential benefits in terms of flow-field modification upstream of high-speed engines were realizable. Much of this work was originally done by Chris Marley at the Missouri University of Science and Technology. This section reports on the results of this initial proof-of-concept investigation. Figure 4.1 show the geometry which was defined here; this geometry was designed specifically to model a very simple high-speed configuration in order to illustrate the phenomena of energy choking and 'engine' unstart. Specifically, this geometry is a constant area (two-dimensional) duct placed in a Mach 10 airstream. Energy in the form of block heat addition across the span of the duct is added to the system between the two parallel flat plates which define the duct (as shown, although due to symmetry, a duct centerline symmetry boundary condition was used such that only one plate needed to be modeled). This situation in terms of the modeling of heat addition corresponds to the analytical case of Rayleigh heat addition (one-dimensional inviscid heat addition), although the flow is modeled here using 2-D CFD (hence incorporating boundary layer and multi-dimensional effects). (An expanded discussion of computational techniques used and the CFD code used will be provided in the following sections). For this preliminary proof-of-concept study, a parametric study is defined such that for a fixed amount of heat rate introduced into the duct (1 Megawatt), the incoming Mach number (free-stream Mach number) is reduced from an initial value of 10 (with freestream temperature and pressure corresponding to a standard altitude of 30 km) until unstart of this simple duct occurs.

Unstart was observed to occur at freestream Mach number of 6 (see Figure 4.2, which plots Mach number contours for this unstarted case).

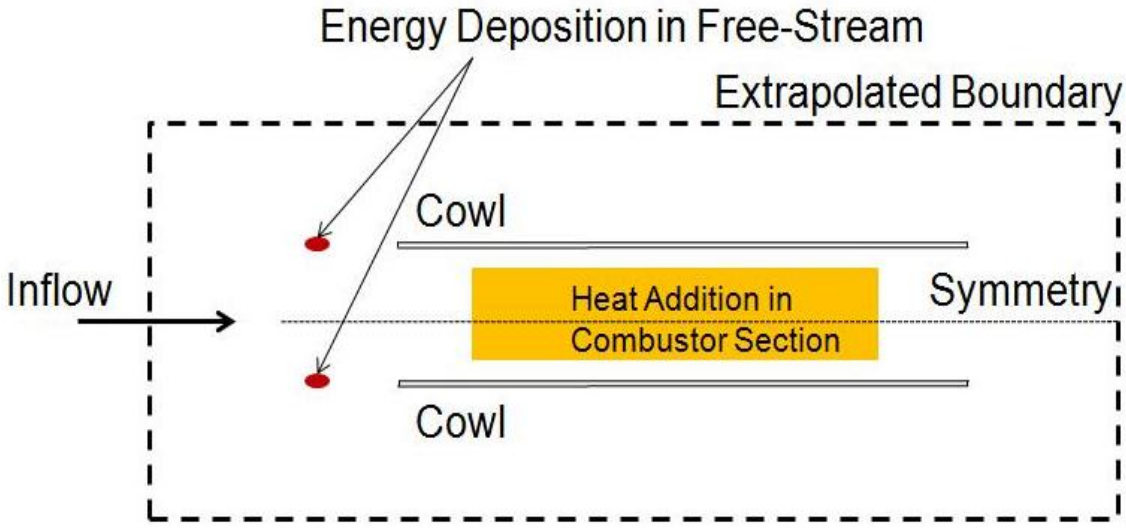

Figure 4.1. Depiction of geometry used for initial analysis of unstart

As can be seen in Figure 4.2, a normal shock is present at the inlet face with associated mass spillage indicated by the turning of the streamline traces. Once the configuration had been unstarted as described, energy was then deposited in a small zone upstream, directly in line with the cowl leading edge. Maintaining the initial condition of an inflow Mach number of 6.0, energy in the constant-area section was reduced to 700kW and 200kW was deposited upstream. The results of this can be seen in Figure 4.3.

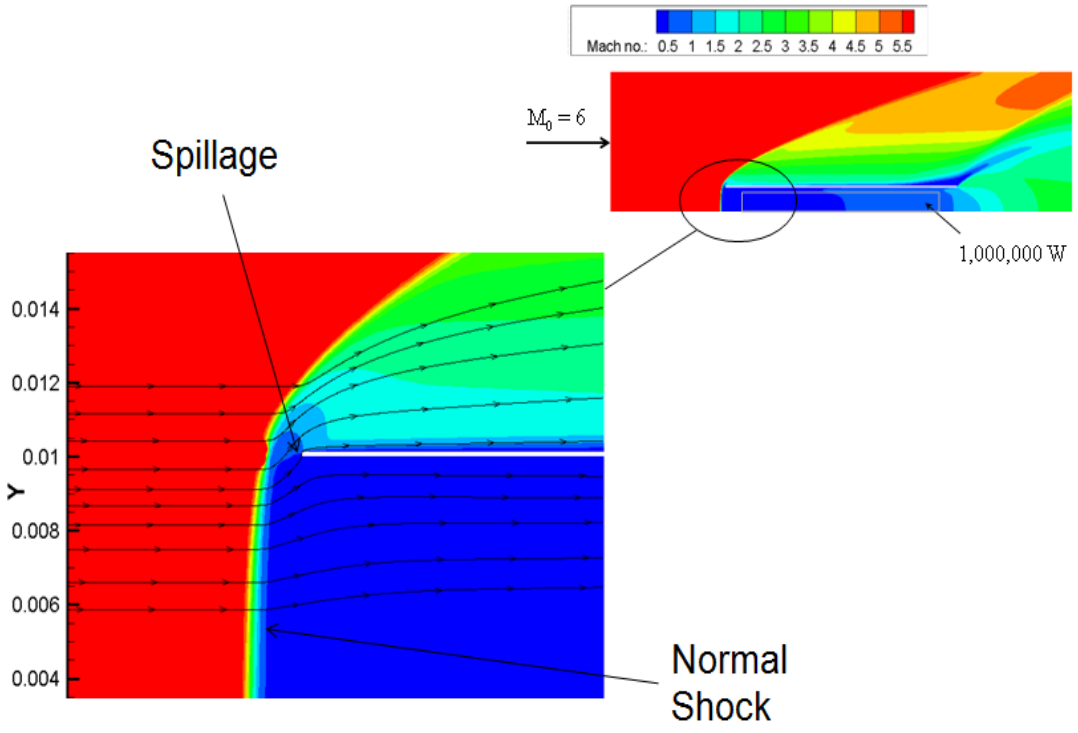

Figure 4.2. Visualization of unstart with 1MW heat addition rate in the constant area section and Mach 6 inflow

In Figure 4.3, beginning with I=0 iterations, the flow along the centerline is subsonic, corresponding to the initially unstarted condition. After the energy deposition upstream, the flow eventually stabilizes at a condition in which supersonic flow is maintained throughout the duct, at least along the centerline of the duct. This preliminary study which clearly demonstrates a recovery from an unstart condition (albeit for a highly simplified situation) provides the impetus to further examine the use of energy deposition for the potential mitigation of unstart (and delay of unstart) and recovery from unstart utilizing a realistic and more complex engine configuration.

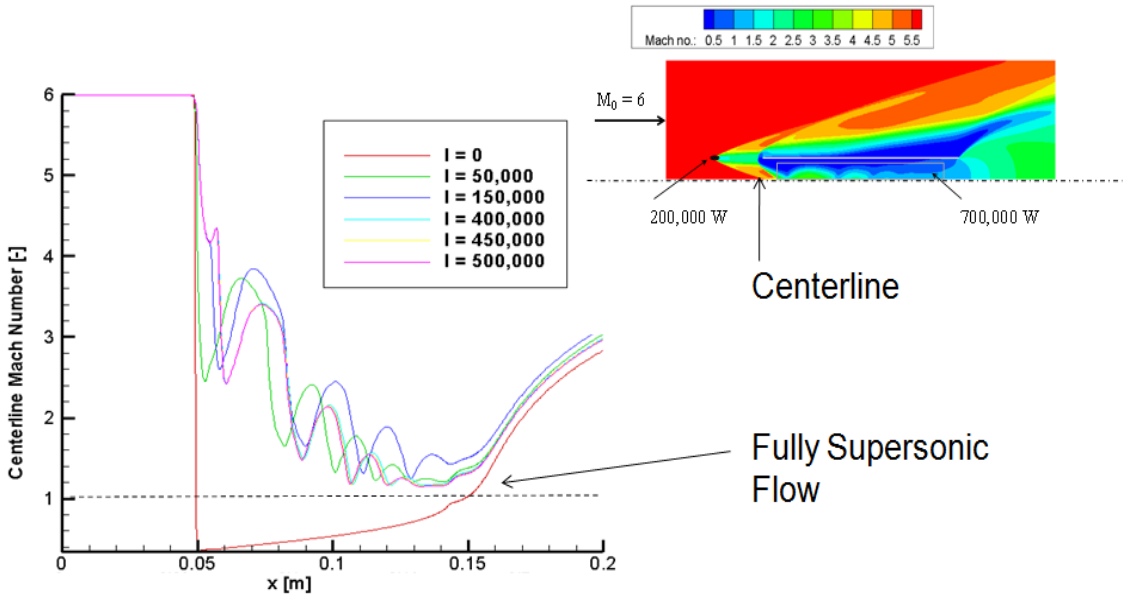

Figure 4.3. Result of using 200kW of energy deposition on an unstarted configuration. Starting with I=0 iteration and progressing through I=500,000 iterations.

5. DEFINITION OF GEOMETRY DEFINED FOR HYPERSONIC VEHICLE STUDY

This section will cover the geometry used for the current study and the initial conditions of the freestream flow. A survey of representative geometries for hypersonic airbreathing propulsion (scramjet and dual-mode ram/scramjet) systems can be found in several basic texts, most notably Heiser and Pratt [9] and Curran and Murthy [10]. Based on these references and previous work, a simple sub-scale 2-D geometry was defined representative of a hypersonic air-breathing vehicle configuration. This geometry is shown in Figure 5.1; it is used for the remainder of the current study.

In order to focus the available numerical resources, the domain of interest for use in the CFD modeling effort encompasses only the engine region itself (as shown in Fig. 5.1). Specifically, the control volume used in the simulation encloses the downstream section of the inlet, the entire engine including the flow beneath the flat-plate cowl, and the forward part of the nozzle/afterbody of the vehicle. Also shown in Figure 5.1 are dimensions and angles of the geometry, approximate locations of heat addition into the domain, and inflow conditions into the modeled domain. Note that based on this definition of the domain of interest, the inflow plane to the modeled region is downstream of the oblique shockwave coming off of the leading edge of the vehicle such that the (post-shocked) inflow conditions into the CFD domain are uniform.

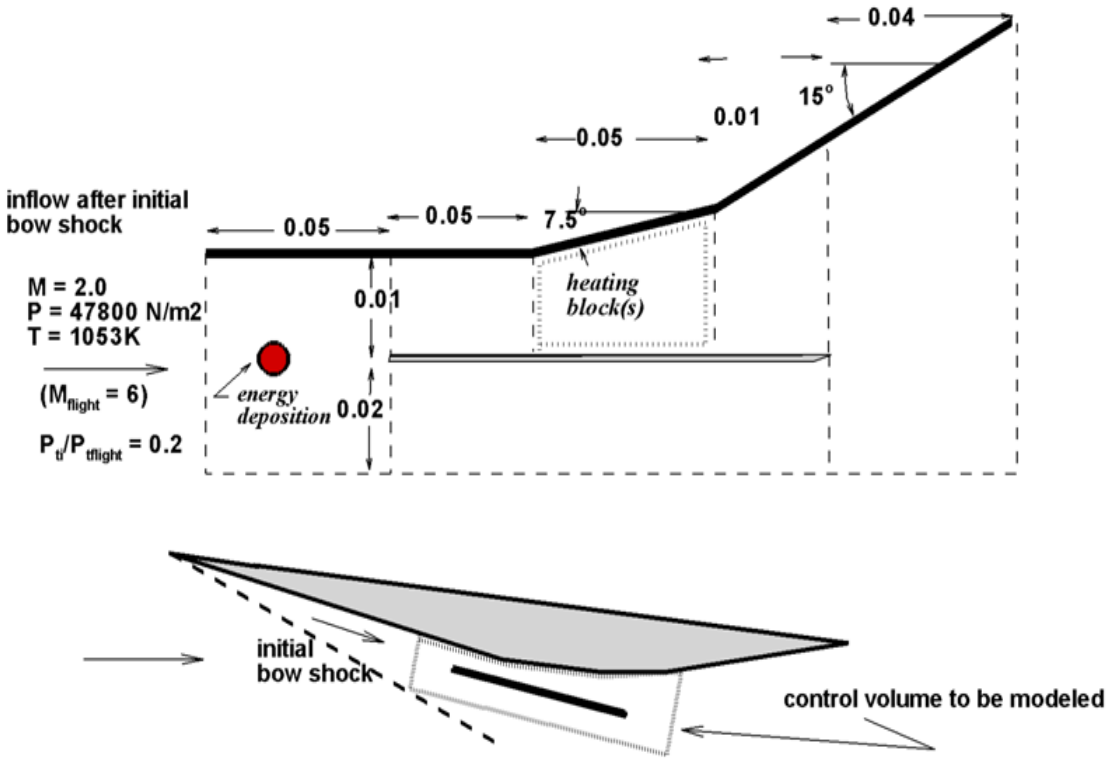

Figure 5.1. Depiction of geometry of control volume used for analysis. All measurements shown are in meters.

These inflow conditions are as shown in the figure and correspond to a freestream (flight) Mach number of 6.0 and an adiabatic total pressure recovery (through the bow shock of 0.2). This model is considered to capture the major features of a hypersonic vehicle which are of interest in the present study. Beginning at the leading edge of the cowl, captured air flow will pass through an internal isolator section before entering the expanding area combustor or burner section (in which the heat release associated with chemical reaction between fuel and oxidizer will be modeled utilizing 'heating' blocks as seen in Figure 5.1). These heating blocks (uniform volumetrically based heating zones which are modeled via a simple source term in the energy equation within the CFD

solver) span the combustor vertical dimension and extend from combustor entrance (isolator exit) to combustor exit. The engine flow then passes through an expansion section, flows over the cowl trailing edge and into the afterbody region as shown. The control volume is extended both upstream of the isolator and downstream of the expansion as well as below the cowl to ensure that all internal and external effects of heat release-induced back-pressurization within the flowfield are captured.

6. CFD CODE DESCRIPTION

This following section discusses the CFD code and assumptions made in the solver. As this study was a numerical investigation, it is necessary to discuss the software and techniques involved in solving the flowfield. The numerical analysis is performed using the VULCAN (Viscous Upwind aLgorithm for Complex flow ANalysis) CFD code (version 6.0.2) ([11] and [12]). VULCAN was developed at the NASA Langley Research Center and is a highly validated finite volume structured grid flow solver for use in high-speed internal and external flows. It can model either calorically perfect gases or a mixture of thermally perfect gases with both equilibrium and non-equilibrium reactions. It solves either the inviscid or fully viscous Navier-Stokes equations, incorporates both space and time marching solvers and an array of turbulence models and has the option to model energy deposition (as used here) via the simple expedient of providing a source term in the energy equation at user-selected grid points or domain regions. VULCAN has been validated for a variety of cases relevant to the present study, notably studies by Rodriguez et al. ([13] and [14]), Cutler and White [15], and Rodriguez, White, and Riggins [16]. For the present study, the air is modeled as thermally perfect with frozen chemistry and is comprised of nitrogen (N_2) (mass fraction of 0.7686) and oxygen (O_2) (mass fraction of 0.2314). As previously mentioned, since frozen chemistry is assumed combustion will be modeled using heating blocks. The Menter SST turbulence model [17] is used based on favorable results in previous similar work and favorable correlation to experimental data in challenging flowfields.

In order to perform a CFD analysis on the defined domain, the geometry is subdivided into seven zones in order to facilitate the parallelization capability of the VUCAN CFD code used in this study as shown below in Figure 6.1. The grid is generated for all blocks utilizing GridGen software and utilizes point-wise boundary point connectivity with clustering at all solid walls. Total grid across all seven blocks or zones incorporates 2000x308 nodes. Note that the cowl is exceedingly thin (thickness of 0.002m or less than 7% of height of control volume) and blunt (rectangular) leading and trailing edges (i.e. it is not rounded).

Figure 6.1. Depiction of zones to make up the control volume for the CFD software.

Upstream (focused) energy deposition, when appropriate for the study, will be in zone 1. Two locations for deposition will be evaluated. The first will be located along the stagnation streamline approximately 0.015 m upstream of the leading edge of the cowl. A second location, approximately 0.008 m from the leading edge of the cowl, will also be examined. Zone 7 is inclusive of the isolator whereas zone 6 is the combustor (or burner) where the 'combustion zone' heating blocks are located. Zones 4 and 5 are

inclusive of the expansion regions aft of the combustor and zones 2 and 3 encompass the flowfield below the cowl.

As mentioned above, in order to minimize the computational requirements necessary for this the combustion-induced heat release in the combustor or burner section will be modeled here using heating blocks rather than modeling actual fuel injection and reaction (seen depicted in Figure 6.2). A similar approach was used by Riggins, Tackett, Taylor, and Auslender [18] and has proved useful for studying unstart effects in high-speed engines. A comparison of entropy generated using finite rate chemistry versus a similar heating block approach showed a high degree of correlation in that same study mentioned above. Figure 6.2 shows the distribution of total heat rate deposited into the combustor component in this study. Specifically, the first block has the greatest heat release rate at 50% of total heat rate, with each subsequent block descending in heat rate received as shown. This approach models to an acceptable degree the actual combustion efficiency distribution associated with fuel injection, mixing and reaction in a scramjet combustor (see [18]).

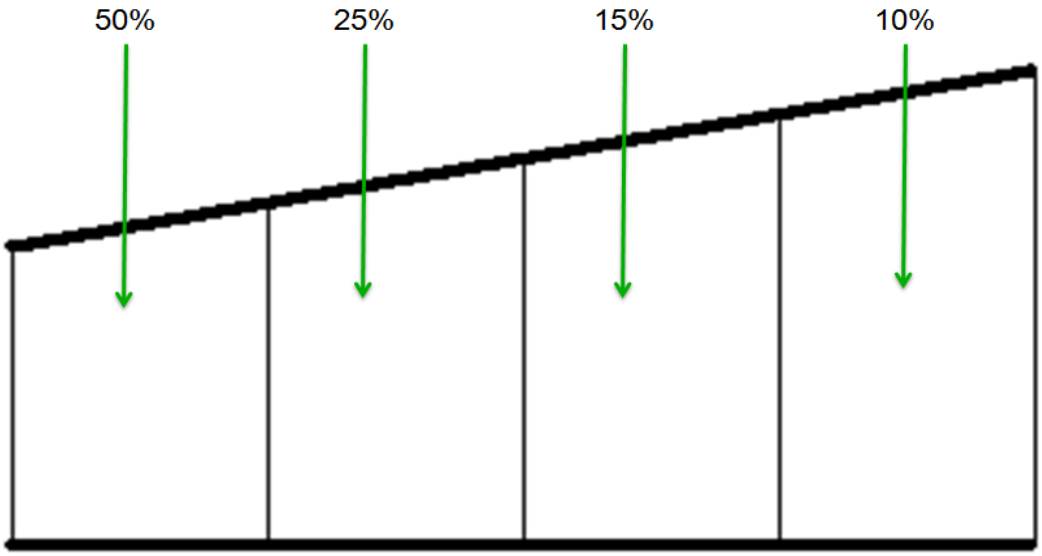

Figure 6.2. Distribution of rate of heat release in the combustor. The first section will receive 50% of the total heat rate in the combustor, the second section 25%, and the last two sections 15% and 10%, respectively.

7. QUASI-ONE-DIMENSIONAL MODELING OF DUCT GEOMETRY WITH HEAT RELEASE

In order to provide an initial assessment of the flowfield before multi-dimensional CFD modeling was done and in order to determine (approximately) an estimate of the amount of energy required to unstart the engine in this geometry, a quasi-one-dimensional analytical differential solver was written. The code was written in MATLAB and solved the following governing equations for mass, momentum, and energy conservation using a simple Euler explicit marching technique [19] technique:

$$\iint_S \rho(\vec{V}\cdot\hat{n})dS = 0 \tag{2}$$

$$\iint_S \rho\vec{V}(\vec{V}\cdot\hat{n})dS + \iint_S P\hat{n}dS = -\tau_w \cdot c \cdot dx \tag{3}$$

$$\iint_S \rho(e+\tfrac{u^2}{2})(\vec{V}\cdot\hat{n})dS + \iint_S P(\vec{V}\cdot\hat{n})dS = \delta\dot{Q} \tag{4}$$

These assume a quasi-one-dimensional flow comprised of a thermally perfect mixture of gases. No work is done on the flow and the heat added will be used to model the combustion. From here, the equations are reduced to a set of differential equations as follows:

$$\frac{d\rho}{\rho} + \frac{du}{u} + \frac{dA}{A} = 0 \tag{5}$$

$$\frac{d\rho}{\rho} + udu = -\frac{\tau_w \cdot c \cdot dx}{\rho A} \tag{6}$$

$$dh + udu = \delta q \tag{7}$$

$$\frac{dP}{P} = \frac{d\rho}{\rho} + \frac{dT}{T} + \frac{dR}{R} \tag{8}$$

This set includes Eq. (8), the differential form of the equation of state. From this set of differential equations, the following set of equations is solved.

$$dh = \sum\{\alpha_l \times C_{p_l} \times dT + h_l \times d\alpha_l\} \tag{9}$$

$$\frac{u_2^2}{2} = \frac{u_i^2}{2} + \delta q - dh \tag{10}$$

$$\rho_2 = \frac{\dot{m}}{(u_2 \times A_2)} \tag{11}$$

$$P_2 = \rho_2 \times T_2 \times R_2 \tag{12}$$

$$P_2 = P_1 + \rho_1 \times \left\{ \frac{-\tau_w \cdot c \cdot dx \cdot u_1}{\dot{m}} - \frac{u_2^2}{2} + \frac{u_1^2}{2} \right\} \tag{13}$$

where

$$h_1 = h_{o_1} + \int_{T_{Ref}}^{T} C_{p_1} \times dT \tag{14}$$

The following provides a description of the solution strategy, assuming a known inflow and geometry: A temperature at the end of the first differential step is assumed. From this assumed temperature, a differential enthalpy can be calculated from Eq. (9). $\frac{C_{p_1}}{R}$ from Eq. (9) is modeled using McBride polynomials. Using the calculated differential enthalpy from Eq. (9), the velocity at the end of the step can be found using Eq. (10). Assuming steady flow, the continuity equation (Eq. (11)) can now be used to determine the density and this can be used along with the ideal gas equation in Eq. (12) to find the pressure. This pressure is compared to the pressure calculated from solving the momentum equation (Eq. (13)). The original assumed temperature is iterated until the pressures calculated in Eq. (12) and Eq. (13) are within a predetermined tolerance. This process is then repeated for each differential step, marching through the internal duct. The solver is set up to model three sections. First, there is a constant area isolator section, followed by a burner section with heat addition, and finally an expansion section. The amount of heat added in the burner section is increased parametrically until Mach 1.0 is first achieved in the burner section (beyond which the quasi-one-dimensional solution technique fails, i.e. it becomes unstable at the sonic point). This relationship between rate

of heat addition and Mach number at the exit of the burner can be seen in Figure 7.1. Figure 7.2 shows Mach number plotted against axial position for 3 megawatts (MW) heat addition rate to the burner.

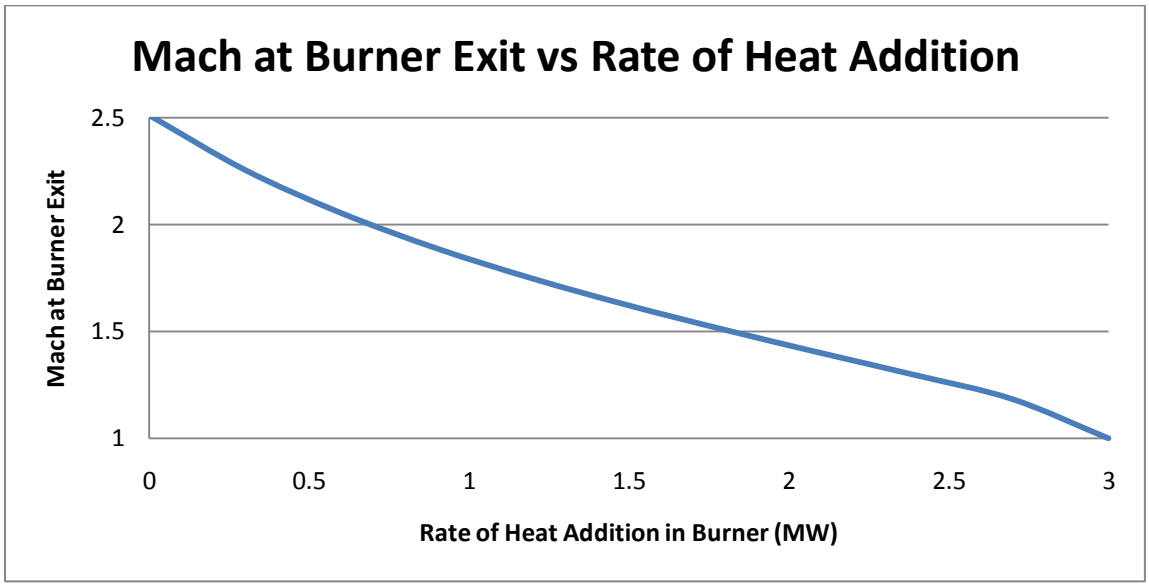

Figure 7.1. Plot depicting the relationship between rate of heat addition in the burner and Mach at the burner exit.

The flow at the entrance to the isolator (beginning of cowl) is initialized at the given inflow conditions (Mach 2.0). The flow is then marched through the isolator (2500 axial steps are taken in the isolator). In the case shown, the total rate of heat addition is evenly distributed throughout the burner section rather than relying on the variable (distributed) heating block approach defined for the CFD. For the case of 3 MW the Mach is driven to 1.0 at the end of the burner section. This provides a reference point in terms of an approximate amount of heat required to unstart the flow for the CFD analysis utilizing the VULCAN CFD software.

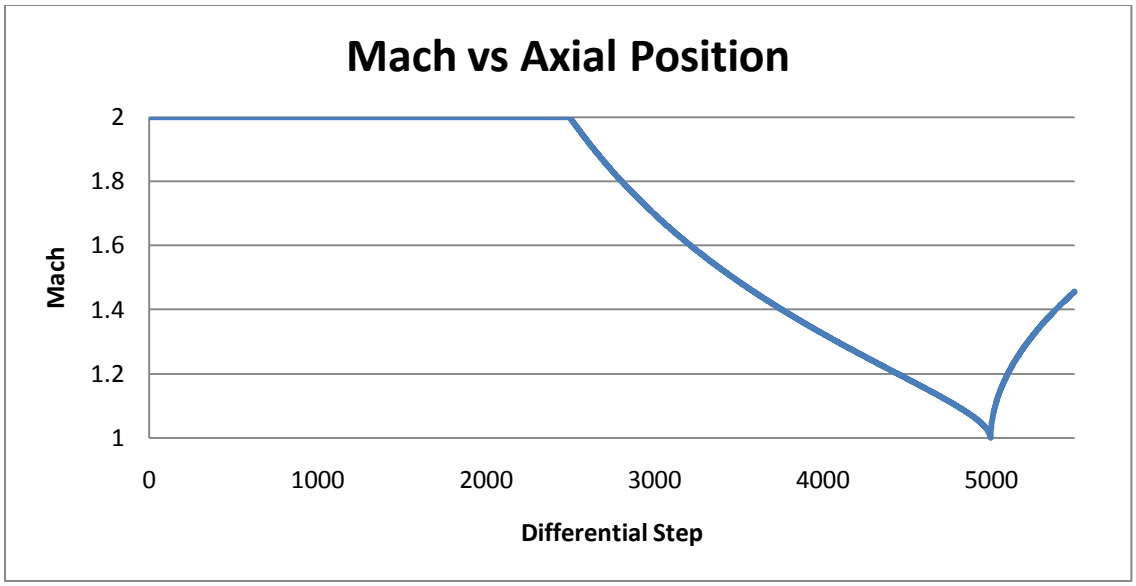

Figure 7.2. Plot of Mach number versus axial position for differential step solver with 3MW heat addition in the burner section.

Based on the inflow conditions as noted in Figure 5.1, the mass flow rate entering the isolator section is 2 kg/sec. A heat-release corresponding to 3 megawatts (MW) in the burner section therefore provides the initial (analytical) estimate of the combustor heat rate required to choke the flow and, hence, begin the unstart in the actual flow. Note that this is an estimate only (and probably very conservative), since the quasi-one-dimensional solver cannot generate the upstream relieving interactions in the isolator which result in the actual engine geometry. The multi-dimensional CFD, on the other hand, will allow these structures and characteristics to be captured. Also of note, the CFD analysis will model the heat addition in four blocks with the amount of heat allocated as depicted in Figure 6.2.

8. CFD RESULTS

This section provides results of the numerical investigation of energy deposition for operability control of a dual-mode engine as defined in Section 5. Here the Vulcan CFD code was used to model the defined engine geometry both with and without upstream energy deposition.

8.1 BASE-LINE THERMAL CHOKING STUDY IN SCRAMJET ENGINE (NO UPSTREAM ENERGY DEPOSITION)

The initial parametric study involved modeling various overall amounts of heat release rates in the combustor section (using a distribution of 4 heating blocks as defined above in Fig. 6.2) with no upstream energy deposition. Figure 8.1 shows the progression of the resulting flow-fields in terms of contours of Mach number, starting with the heat rate required to achieve thermally choked flow as obtained utilizing the quasi-one-dimensional solver – see last section) in Figure 8.1a (3 MW in the combustor) through the fully unstarted flow in Figure 8.1f (corresponding to 8MW in the combustor as depicted in Figure 8.1f). In Figure 8.1a, the classic shock train can be seen in the isolator section as well as the beginnings of a separated boundary layer along the upper surface along the body. Figure 8.1b (for 4MW in the combustor) displays a marked growth in the separation layer along the body on the upper surface and an increase in the number of shocks within the shock train in the isolator. Figure 8.1c (for 5MW in the combustor) demonstrates incipient unstart. A normal shock extends from the leading edge of the cowl up to the separation layer and ,as can be seen from the stagnation streamline (defined as the streamline which terminates on the leading edge of the cowl), there is a

large amount of mass spillage from the inlet face. This case of 5MW in the combustor with no upstream energy will be considered the baseline case for the rest of this study. Figures 8.1d through 8.1f are for 6MW, 7MW, and 8MW (heat release rates) in the combustor, respectively. The progression in these figures clearly shows continued growth in the separation layer and increased mass spillage. Ultimately, the 8MW case (Figure 8.1f) shows complete mass spillage (i.e. the mass capture into the engine is 0%). Here, the entire isolator section is simply filled with recirculating flow. It should also be noted that Figures 8.1d through 8.1f are only run for 10,000 iterations and hence may not fully represent convergence in time. They are included in order to show (visually) the full progression of engine flow-fields to complete unstart, following the development of incipient unstart. For evaluation of the potential of energy deposition for use in mitigating and recovering from unstart, the 5MW case as shown in Figure 8.1c (exhibiting incipient unstart) will be used as the baseline reference case for all following cases which utilize upstream energy deposition. It should be noted that for the following cases using upstream energy deposition, multiple configurations and energy levels were studied. The cases depicted in the following figures and discussion represents the minimum energy levels and locations necessary to affect the flow adequately.

8.2 UPSTREAM ENERGY DEPOSITION FOR FLOW-FIELD MODIFICATION

As has been previously stated, work by Shneider, Macheret, Zaidi, Girgis and Miles [7] from Princeton has shown the potential for a ‘virtual cowl’ concept in which a very large amount of energy is deposited just below the cowl line in order to increase mass capture.

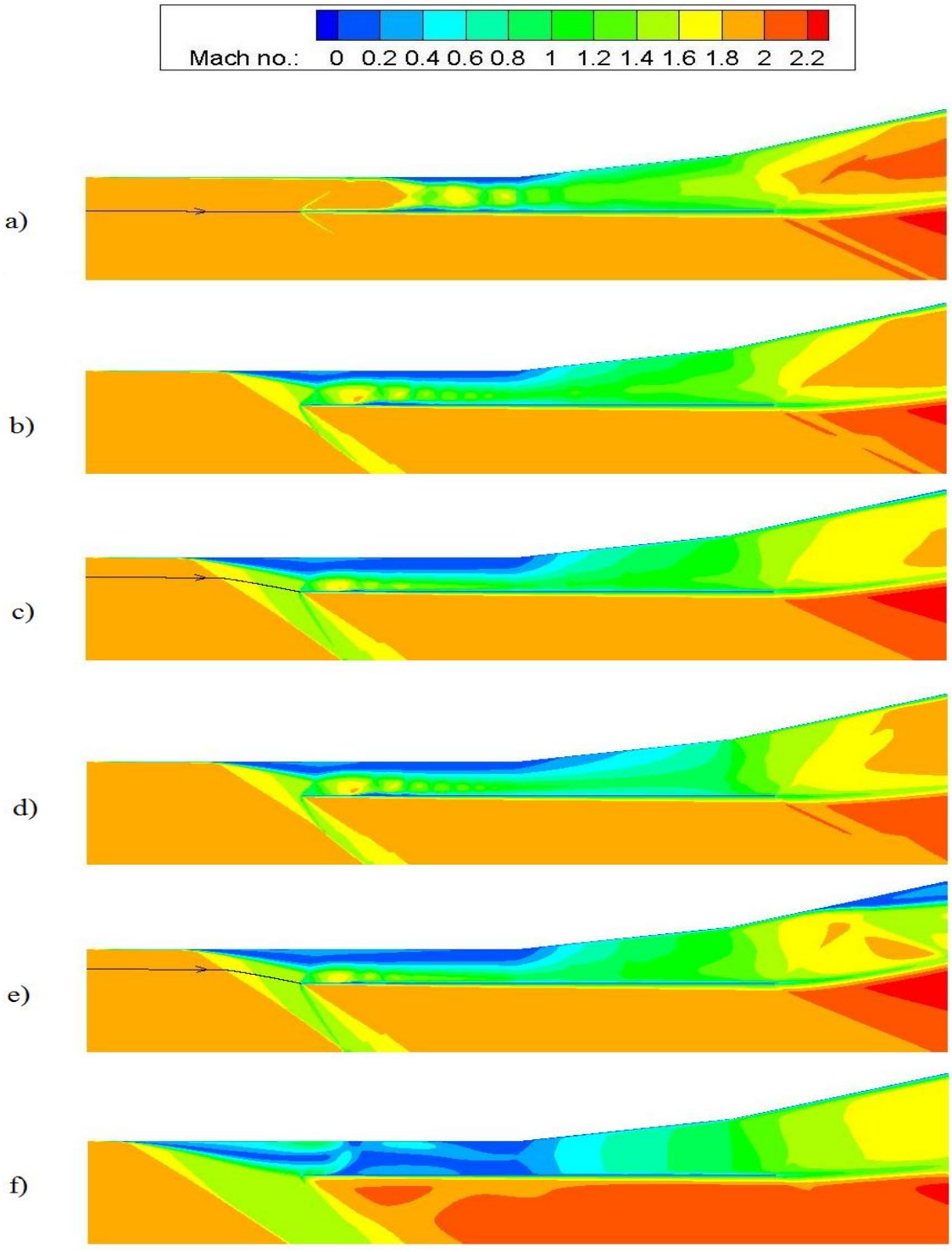

Figure 8.1. Display of the progression of flowfield Mach number from thermal choking through unstart using energy deposition (power) in the burner section. Cases shown are for a) 3MW, b) 4MW, c) 5MW, d) 6MW, e) 7MW, and f) 8MW deposited in the burner.

However, work by Riggins, Nelson and Johnson [4] displayed significant fluid dynamic interaction between the energy deposition region and a blunt body structure located downstream, when relatively modest amounts of energy was deposited along the stagnation streamline. As such, the focus of this study will look at energy deposition along the stagnation streamline. Note that studies by Bisek, Boyd, and Poggie [5] have showed the independence of shape of energy deposition on drag reduction (although this result is not universally accepted). In this study, the shape of the upstream energy deposition zone will take either of two forms, as depicted in Figure 8.2 The energy deposition zone denoted 'block deposition' is comprised of a region in the flow which forms (approximately) a square utilizing a 14x14 block of nodes. The energy deposition zone denoted 'streamline deposition' is a higher-aspect ratio rectangle oriented in the flow direction (approximately) along its longer axis. The streamline deposition covers 40x5 nodes in the flowfield. Both of these shapes are centered along the stagnation streamline.

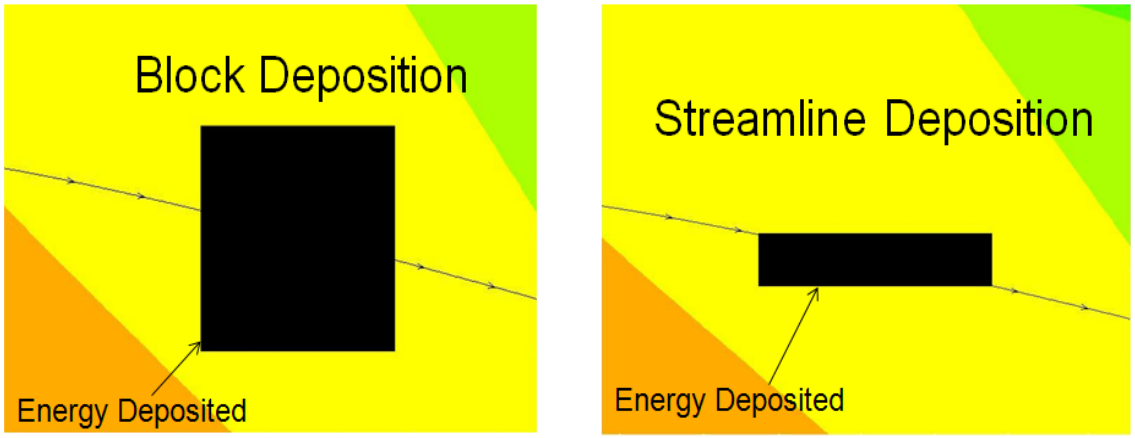

Figure 8.2. Geometry of upstream energy deposition. As shown, the left shows a block deposition case while the right shows a streamline deposition case.

The first case examined corresponds to 5 MW heat addition rate in the combustor section along with 500 kW deposited upstream along the stagnation streamline for both zone shapes. Figure 8.3 shows the results of the flowfield in terms of Mach number contours for both zone shapes. In both of these contour plots, the initial condition used for the flowfield modeling was freestream, i.e. inflow flow conditions were assumed across the entire domain. Therefore, energy deposition is used in this case in the attempt to prevent unstart from occurring or mitigating its effects should it occur. It should be noted that while the upstream deposition of 500 kW represents 10% of the energy rate supplied in the combustor (and hence seems large as compared to energy deposition rates required for previous drag reduction studies as discussed earlier), the flow static temperature (where energy is being deposited) for this configuration is over 1000 K. In order to effect useful coupling between the energy deposition zone and the cowl leading edge, a sufficiently large amount of energy is necessary to sufficiently raise the temperature of this high-temperature flow and lower the Mach number in and downstream of the energized zone to interact with the cowl.

As can be seen in Figure 8.3a, even with 5MW in the combustor (which recall results in unstarted flow without upstream energy deposition), the addition of the 500 kW of energy upstream and attendant flow-field effects prevents the formation of a normal shock at the inlet and actually improves mass capture when compared to the baseline case shown in Figure 8.1c. Figure 8.3b shows similar results to Fig. 8.3a except the energy deposition zone shape corresponding to the streamline deposition is used. As Figure 8.3b shows, the streamline deposition also prevents the formation of a shock wave at the inlet and improves mass capture.

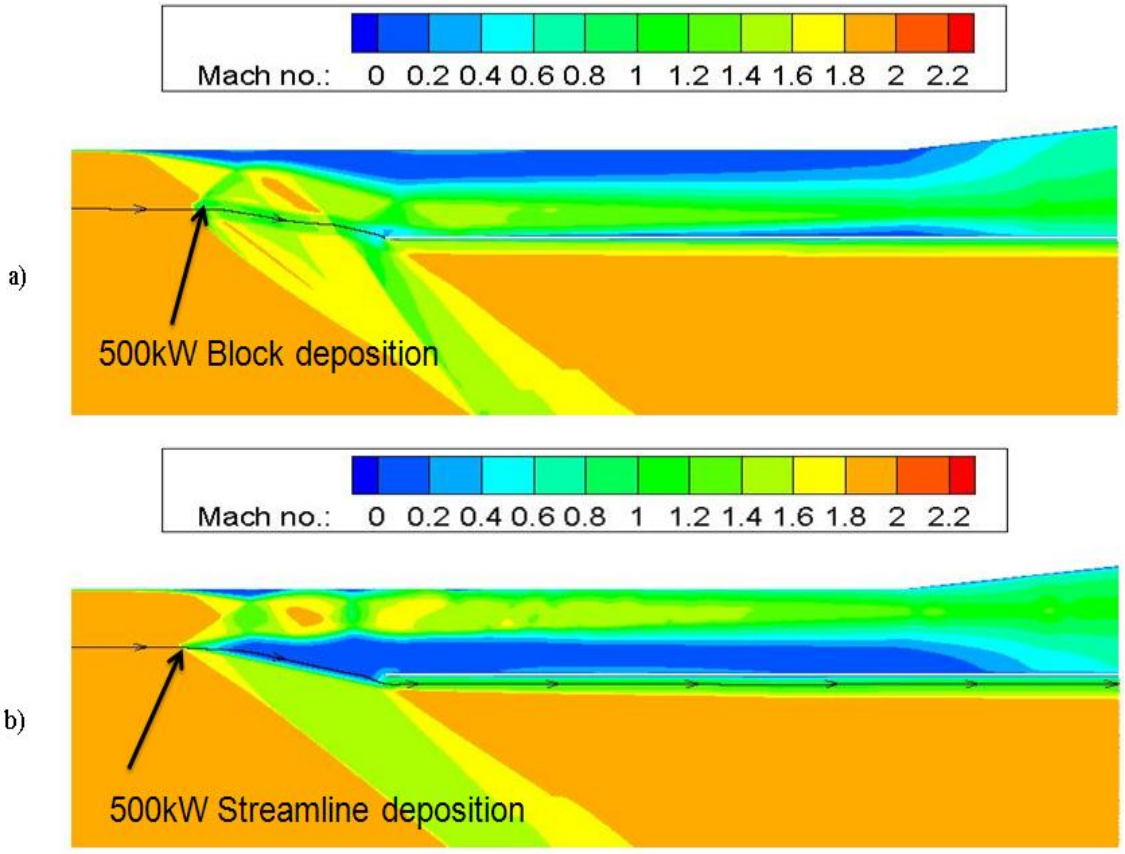

Figure 8.3. Comparison of 500 kW cases with freestream initial condition. In a), a block deposition is used to mitigate unstart, while in b) a streamline deposition is used.

But also of note is the massive flowfield modification achieved with the streamline deposition (zone shape) case in which there is massive coupling between the energy deposition zone and the cowl leading edge. The separation layer which had originally formed along the upper boundary on the body is now completely shifted to along the cowl and extends upstream all the way to the upstream energy deposition region. Therefore, besides application to the unstart problem as detailed here, there is also potential for a virtual cowl concept utilizing energy deposition as shown here and alluded to before in the literature review section. Note that the main reason for the

massive coupling in the streamline deposition case is the higher temperature and lower Mach number achieved in the energized region along the stagnation streamline.

The next case examined uses the same 500 kW upstream energy rate deposition. However, the initial condition is now chosen as the baseline unstarted case with 5 MW in the combustor, i.e. the object is to attempt and try to restart the engine from an unstarted configuration using upstream energy deposition (recovery from unstart). Figure 8.4 provides contours of Mach number for this case, again with results shown for both block energy zone deposition and streamline energy deposition.

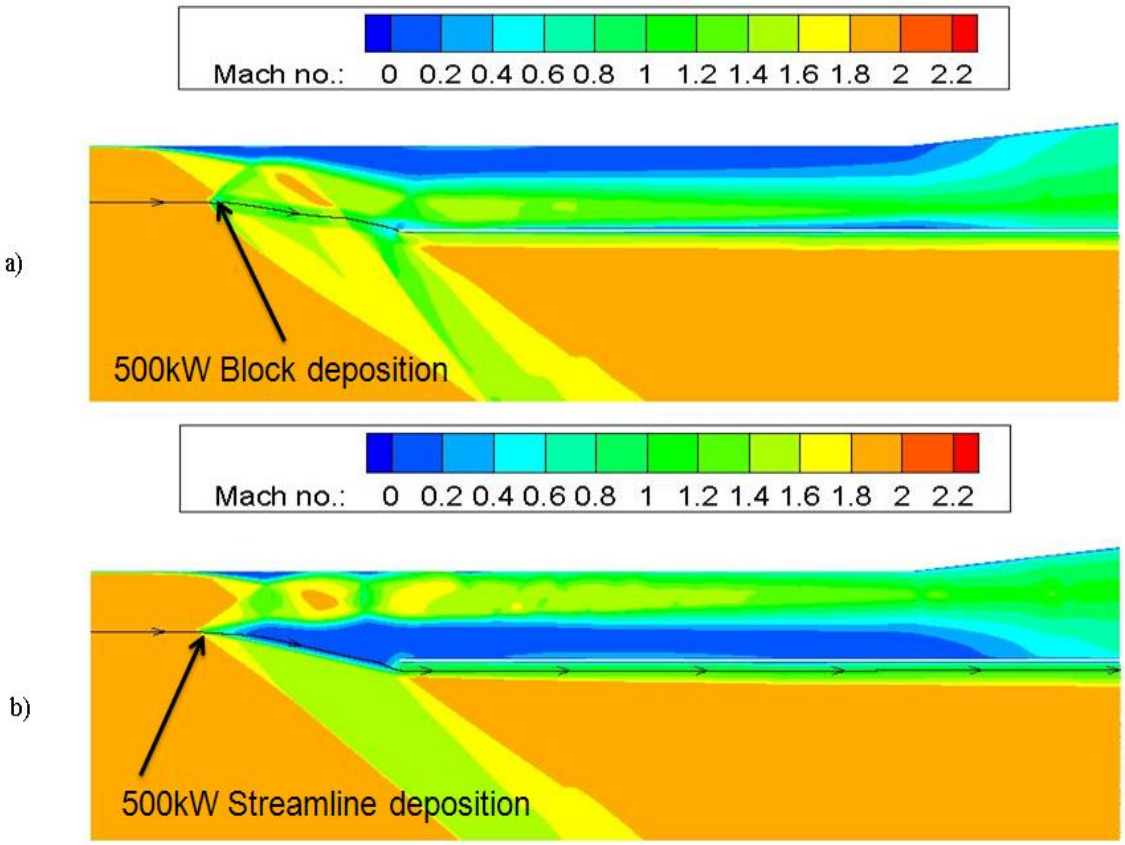

Figure 8.4. Comparison of 500 kW cases with unstarted flow for initial condition. In a), a block deposition case is used whereas in b), a streamline deposition is used. Both cases started from the initial condition of an unstarted engine with 5 MW in the burner.

Both zone shape cases in Fig. 8.4 show a return to started flow from an unstarted condition. As was the case in Figure 8.3, Figure 8.4b also shows the same radical shift in the flow with respect to the separation bubble moving from the upper surface side to the cowl side.

Also of interest is the fact that both cases (involving the mitigation of unstart and the recovery from unstart) stabilize to provide the same flowfield as can be seen when comparing Figure 8.3a and Figure 8.4a or Figure 8.3b and Figure 8.4b. In the case of Figure 8.3a and Figure 8.4a, both techniques prevent a normal shock from forming and both increase mass capture when compared to the baseline case in Figure 8.1c. Note that the Mach contours in both cases are virtually identical.

The next case tested in the present study provides a comparison of the case utilizing 500 kW upstream energy deposition (streamline deposition zone shape) to a case with 200 kW upstream, also utilizing a streamline deposition zone shape. As shown in Figure 8.5 below, both the 200 kW and 500 kW upstream energy deposition cases prevent unstart from occurring. In Figure 8.5b (200 kW upstream energy deposition), it can be seen that the separation boundary layer does not extend nearly as far upstream as the case with 500 kW upstream energy deposition. Also, the height of the separation layer in Figure 8.5b for the 200 kW case is not as large as the height in Figure 8.5a, resulting in an increase in mass capture for the lower energy deposition level. Of note is the fact that this case in which 200 kW of energy was deposited upstream used the converged results of the preceding 500 kW case as its initial condition (i.e., as if the 500 kW was deposited upstream, the flow was allowed to stabilize, and then the upstream energy was reduced to 200 kW).

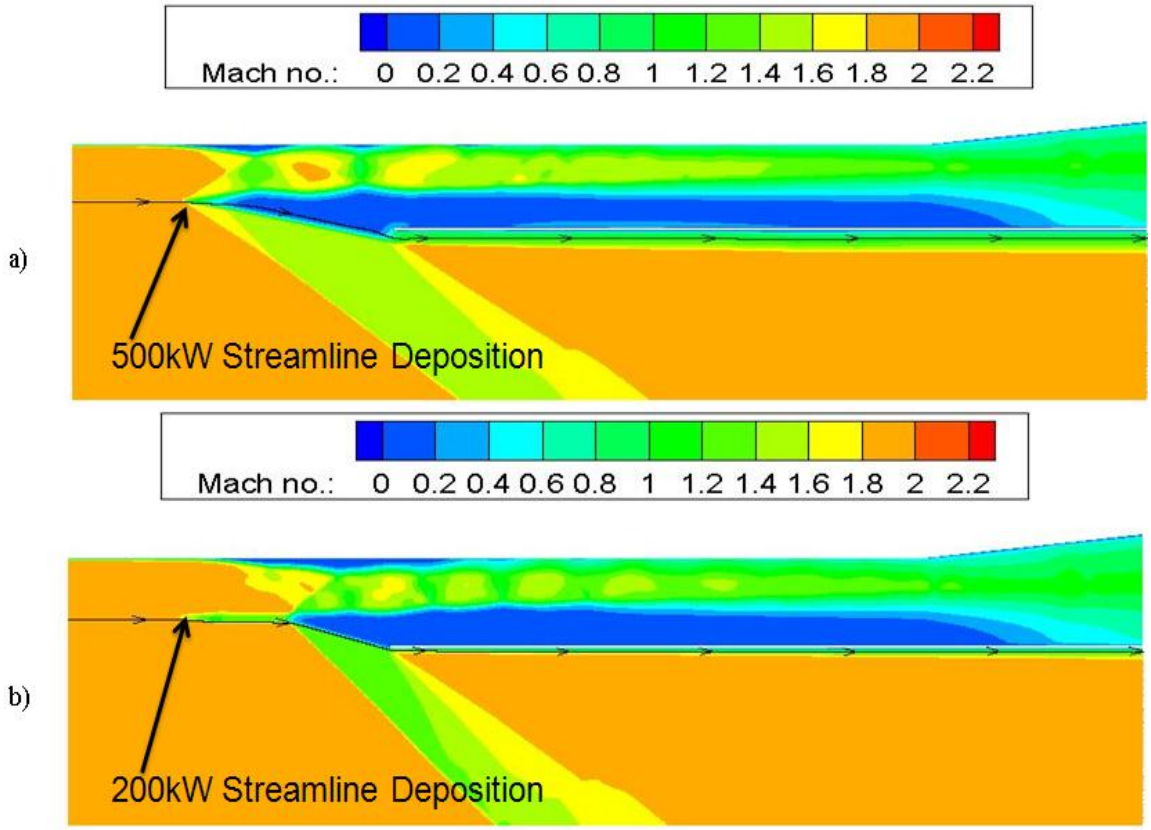

Figure 8.5. Comparison between 500 kW and 200 kW. In a), 500 kW are deposited upstream while in b), 200 kW are deposited.

This case indicates that a steady-state energy deposition rate corresponding to the higher level of 500 kW upstream is not necessary for mitigating unstart.

The next case examined whether the 200 kW deposited upstream could mitigate unstart without using the 500 kW case as an initial condition (i.e. no initial spike of upstream energy required). As can be seen in Fig. 8.6, when the solution is begun using the freestream condition as an initial condition with 5 MW heat release rate in the combustor and 200 kW deposited upstream in the streamline fashion, it is insufficient to prevent unstart from occurring at the inlet. This shows that while the 200 kW upstream deposition is sufficient to maintain started flow following an initial deposition of 500 kW

to restart the flow, it is not enough (on its own) to prevent unstart. It also does not demonstrate the observed flowfield modification in which the separation layer is shifted from the body side to the cowl side. This indicates that using 200 kW of upstream energy addition for unstart mitigation is path dependent and is a function of both upstream energy levels and the initial condition (i.e. to maintain started flow it must follow an initial higher power deposition case.)

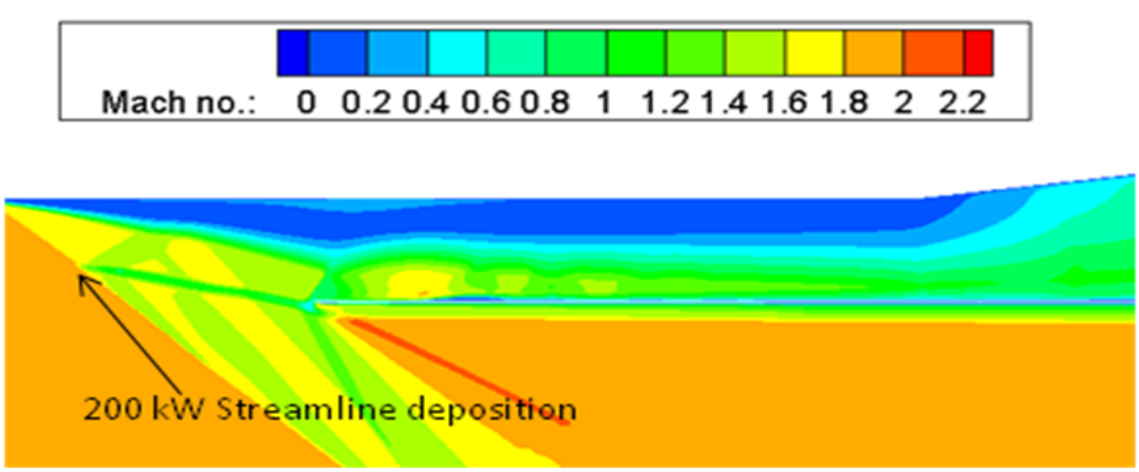

Figure 8.6. 200 kW streamline deposition case beginning from freestream initial conditions with 5 MW in the burner section.

The final case presented here evaluated the effect of the location of the upstream energy deposition region. The deposition region for preceding cases was located approximately 65% downstream of the leading edge of the control volume in (grid block) zone 1 (approximately 0.015 m upstream of the cowl leading edge). In order to enhance possible interaction of this deposition region with the cowl leading edge, it was moved closer to the cowl (to approximately 85% downstream of the leading edge of the control volume in zone 1 or 0.008 m upstream of cowl leading edge) but located still along the stagnation streamline. As can be seen in Fig. 8.7, this maintains started flow but fails to

shift the separation layer from the body to the cowl side, as had been observed in the other streamline deposition cases.

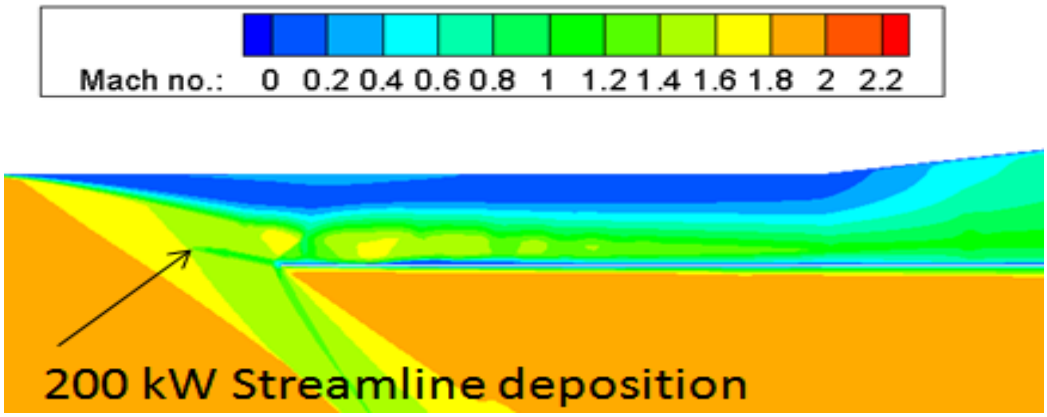

Figure 8.7. 200 kW streamline deposition moved closer to cowl leading edge than previous cases. 5 MW in the burner.

Table 8.1 provides quantified results for a number of the cases discussed in this work. The cases are defined in terms of energy rate in the combustor, the upstream energy rate deposition amount and energy deposition zone geometry, and flowfield initial condition. The key factor is the percentage of mass capture as normalized by full mass capture into the engine. For the cases with no upstream energy deposition, the mass capture continues to drop as energy in the combustor is increased until the case with 8 MW in the burner has zero mass capture. For all upstream energy deposition cases using 500 kW, regardless of flowfield initial condition or deposition zone geometry, the mass capture appears to depend only on the amount of energy deposited upstream. Each of the (upstream energy deposition) 500 kW cases show an improvement of almost 20% increased mass capture over the baseline case of 5 MW in the combustor with no upstream energy . Finally, as previously noted, each of the cases using only 200 kW upstream energy deposition show a small improvement over the nominal baseline case.

Furthermore, the first case using only 200 kW upstream (utilizing the results of the 500 kW upstream case as initial condition) shows an improvement over the 500 kW upstream energy deposition cases in terms of mass capture percentage.

Also shown in Table 8.1 is the calculation of axial force experienced by the solid walls of the engine (within the modeled region) for each of the cases. For all cases shown, the net force due to pressure acting on all wetted surfaces in the control volume was determined by numerically integrating the pressure acting on the area as seen in Eq. (15)

$$F = \int P \cdot dA \text{ where } dA = dA \cdot \hat{n} \tag{15}$$

and taking the axial component of F as follows

$$F_x = F \cdot \sin\theta \tag{16}$$

Here θ is the local angle measured with respect to the cowl. As can be seen in the table, the axial force generated on the body continues to rise as the rate of heat release in the burner is increased until 5 MW is in the burner. At this point, there is a precipitous drop in force generated, indicating this is an "operational cliff", beyond which the engine is unstarted. For all cases in which energy is deposited in the flowfield, either in the burner or upstream, this baseline case represents the minimum amount of axial force produced. Recall that this was the flow-field used as the initial condition for all upstream energy deposition cases. The primary focus of the current investigation was to see if (by utilizing upstream energy) it is possible to either prevent the drop in force altogether or potentially delay the drop in terms of amount of energy, such that more energy could be added into the burner without drastically losing performance. As can be seen from comparing the percent differences between each of the cases compared to the nominal 5

MW case, all cases resulted in both a higher mass flow rate into the inlet as well as more axial force produced. This can also be more clearly seen in Fig. 8.8 and Fig. 8.9 below for force and mass flow rate, respectively.

Table 8.1. Tabulation of cases showing energy in the burner, amount of energy upstream, orientation of upstream energy and initial flowfield condition.

Energy in Combustor (MW)	upstream energy (kW)	Orientation of upstream energy	Initial State	Final State	% of Ideal Mass Flow rate	Local Axial Force (N)	% Difference in Axial Force over 5MW case
0	0	-	Free-stream	started	97.90	947	-14.48
3	0	-	Free-stream	started	98.17	1119	1.09
4	0	-	Free-stream	unstarted	83.19	1254	13.25
4.5	0	-	Free-stream	unstarted	75.01	1291	16.59
5	0	-	Free-stream	unstarted	56.39	1107	0.00
7	0	-	Free-stream	unstarted	56.16	1201	8.42
8	0	-	Free-stream	fully choked	45.20	1236	11.64
5	500	block	Free-stream	started	65.48	1217	9.89
5	500	line	Free-stream	started	64.11	1166	5.31
5	500	block	unstarted	started	65.14	1211	9.36
5	500	line	unstarted	started	64.10	1167	5.34
5	200	line	started	started	66.83	1197	8.13
5	200	line	Free-stream	unstarted	59.23	1128	1.83
5	200	line (close)	Free-stream	started	59.81	1139	2.83

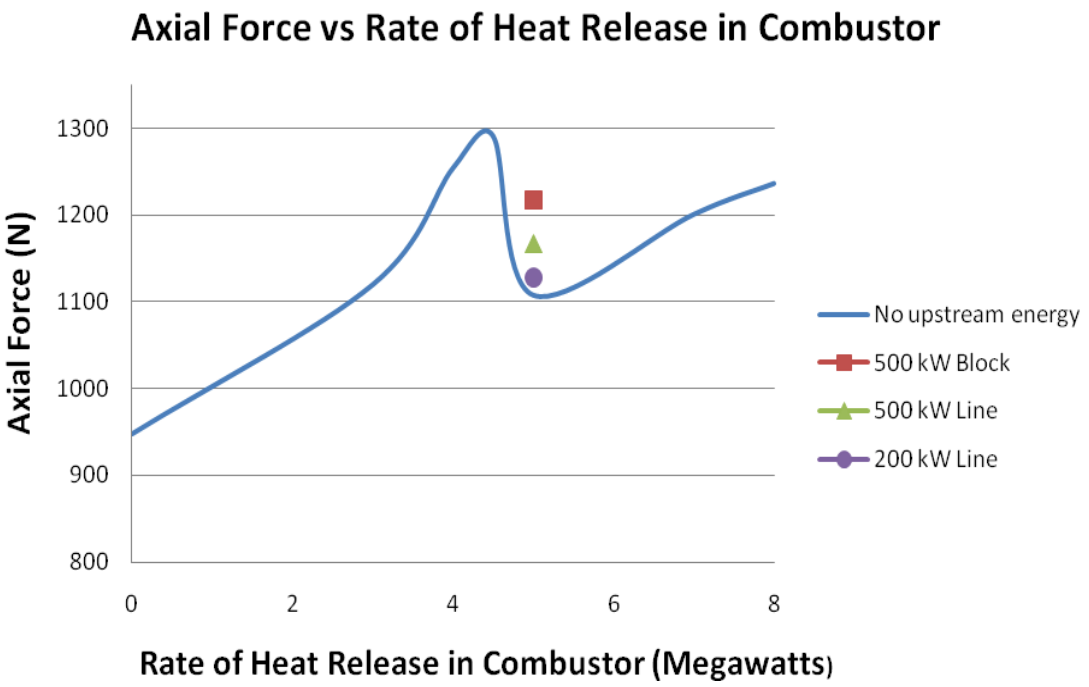

Figure 8.8. Axial force generated plotted against rate of heat release in burner section. Line represents no upstream energy while the singular points depict various amounts of energy deposited upstream with 5 MW in the burner.

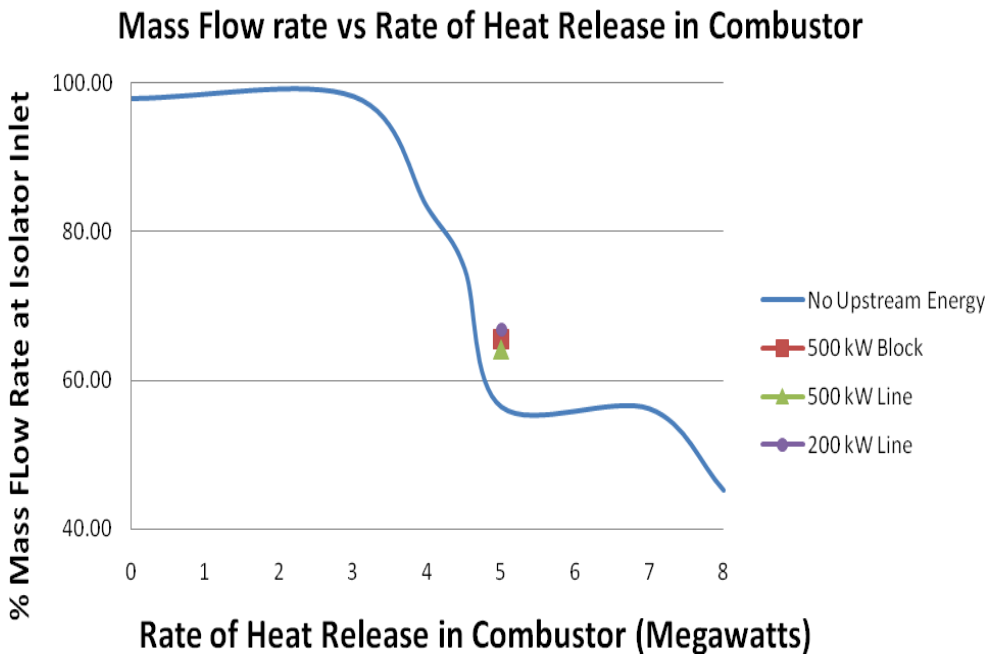

Figure 8.9. Mass flow rate at inlet to the isolator plotted against rate of heat release in the burner. Line represents no upstream energy while the singular points depict various amounts of upstream energy with 5 MW in the burner.

9. GRID AND SOLUTION CONVERGENCE

In order to provide information regarding the temporal and spatial convergence obtained in this numerical investigation, the following provides a discussion of grid refinement study as well as the temporal convergence of the baseline case (i.e. 5 MW in the burner with no upstream energy deposition). The other cases shown in this thesis were observed to have similar convergence behavior. Mass flow rate at the aft end of the cowl was non-dimensionalized by normalizing with the mass flow rate entering the isolator inlet and plotted against the number of iterations as shown in Figure 9.1.

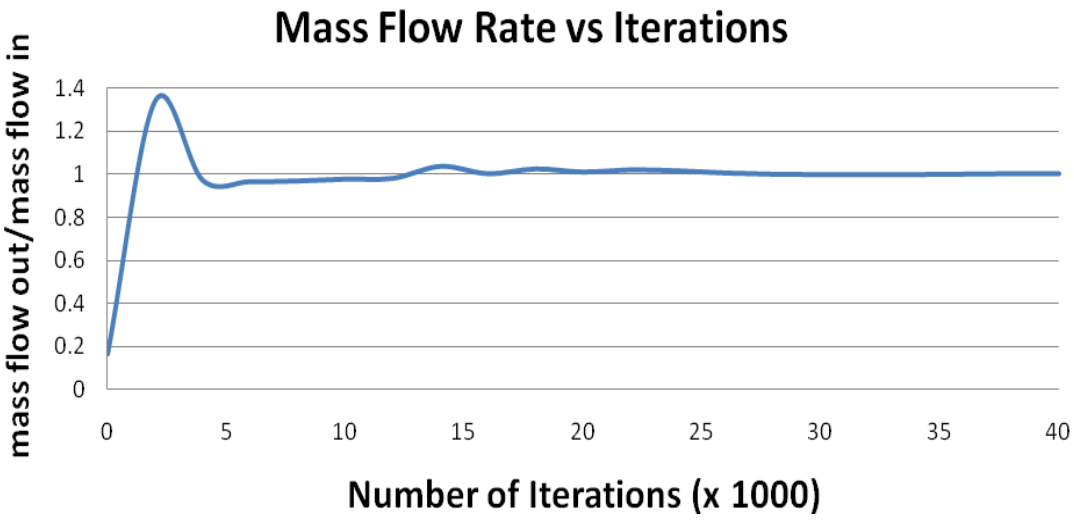

Figure 9.1. Ratio of outflow to inflow mass flow rate plotted against number of iterations for the case of 5 MW in the burner with no upstream energy.

After some early fluctuations, the flow stabilizes after roughly fifteen thousand iterations and particularly so after twenty thousand iterations. All cases using upstream energy deposition analyzed in this study were run for between 20,000 and 30,000 iterations.

In order to assess grid convergence, the base-line grid used for the cases studied (2000 x 308 nodes) is termed here as the medium grid. A coarse grid of 1000 x 154 nodes and a fine grid of 4000 x 608 nodes were then constructed and analyzed using the base-line case conditions. Each was run for a minimum of forty thousand iterations. At this point, the total pressure in the section of the control volume bounded by the body and the cowl was one-dimensionalized by taking the mass-weighted average and then plotted versus the normalized axial distance along the cowl, for all three grid levels. Fig. 9.2 shows the results of the grid convergence study. Up through most of the isolator, the results for the fine and medium grids are virtually identical. While they begin to slightly diverge as the flow enters the burner section (at approximately x/L = 0.5), they both exhibit the same profile throughout both the burner and expansion regions. As such, it is stated here that the medium grid yields satisfactory results in terms of grid convergence – and at great reduction in computational cost for this investigation.

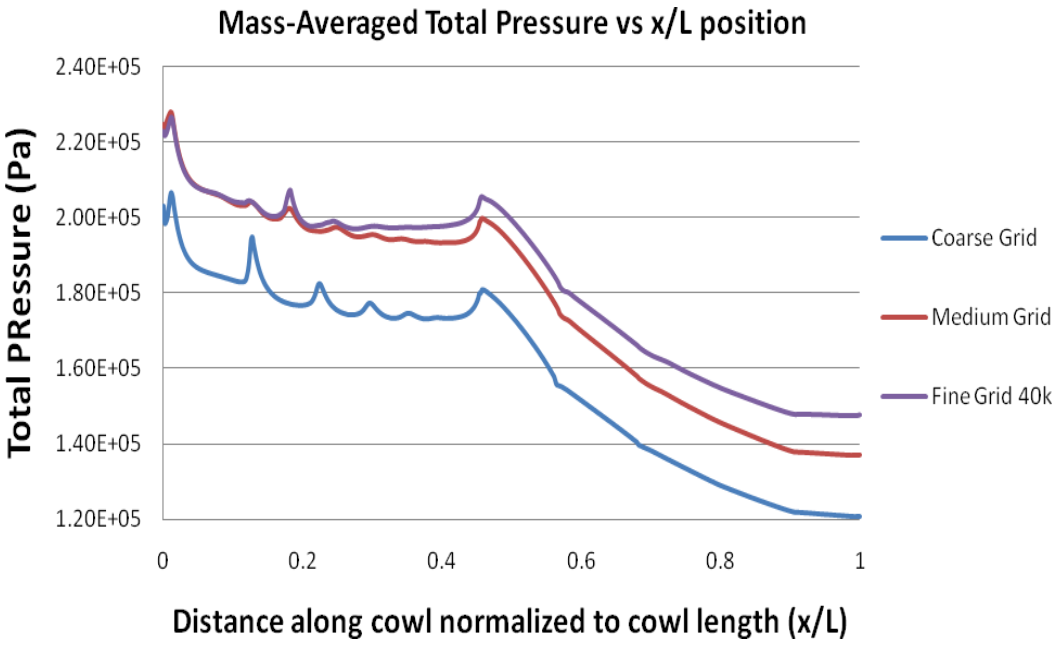

Figure 9.2. One-dimensionalized mass-weighted total pressure plotted against axial position normalized to cowl length through the comprising the isolator, burner and expansion region of the cowl.

10. CONCLUSIONS AND SUMMARY

The cases evaluated have shown that upstream energy deposition has the potential for improving the operating envelope of a dual-mode ram/scramjet engine system with regards to preventing, mitigating or recovering from engine unstart in high-speed flight. This study began with a simple proof-of-concept analysis using basic 2-D duct geometry to evaluate the impact of upstream energy addition on an unstarted engine. Recovery from unstart back to a started condition in that analysis led to further multidimensional CFD work using a more realistic geometry. The results of the analysis from the VULCAN CFD work have shown the potential for applications of upstream energy deposition in a couple of areas. The first was a central (original) focus of this study and displayed the limited ability to both mitigate as well as recover from unstart, although the overall performance was not considerably enhanced due (mainly) to mass capture defects. However, this work suggests a second area: The potential exists to expand the operating envelope of a dual mode ram/scramjet propulsion using energy deposition techniques, especially from the standpoint of controlling the engine flow-field without physical (geometric) changes required in the engine.

It should be noted that the magnitude of energy deposition required for flow modification in front of dual-mode ram/scramjet engines is high (i.e. up to 10% of the rate of heat release in the combustor) relative to earlier studies of energy deposition for drag reduction and control of blunt leading edges. This is due to the higher temperature and density flow (and lower Mach number) flow behind the forebody oblique shock wave (where the energy must be added in front of the internal engine for the application in this

study). Low temperature and low density flows (i.e. in the freestream upstream of the vehicle leading edge) are more amendable in terms of achieving shock wave modification for lower energy amounts. This requirement (depositing energy behind the forebody shock(s) of the vehicle in high temperature and density air) is expected to be a significant disadvantage for the application examined here, since larger amounts of energy must be provided to achieve appreciable flow-field modification.

The most significant positive result from this study was that there is performance potential for further investigation of a 'virtual cowl' concept as shown in the streamline deposition cases in the results section. A review of computed flowfields resulting from streamline deposition of energy show potential massive interactions between the cowl leading edge and the energy deposition region with large scale changes in flow-field character, leading at least conceptually to the possibility of extending a 'virtual' isolator into the upstream flow as well as creating a 'virtual' (non-physical) cowl flap with the interaction between cowl and energy deposition.

Suggested future work would produce, analyze and document results for upstream energy deposition cases in terms of more energy levels besides 500 kW and 200 kW cases as well as a variety of deposition locations other than along the stagnation streamline (i.e. would focus on parametrically varying the energy amount, location and distribution for performance optimization). Thermal issues were not considered in this investigation but are obviously of importance. This study, as mentioned above, does not address the system-level aspects of the subsystems necessary to provide the energy deposition capability; this remains to be done.

Particular attention should also focus on quantitatively evaluating the performance of the ‘virtual cowl’ concept for a variety of free-stream Mach numbers (above and below the Mach 6 freestream flow solely analyzed in the present study).

BIBLIOGRAPHY

[1] Bao, W., Chang, J., Yu, D., Xie, Z., "Optimal Classification Criterions of Hypersonic Inlet Start/Unstart," Journal of Propulsion and Power, Vol. 23, No. 2, March-April 2007, pp. 310-316.

[2] Barnett, J.T., Riggins, D.W., and Taylor, T., "Drag Reduction and Heat Transfer Mitigation for Blunt Bodies in Hypersonic Flight – A Survey of Techniques," AIAA Paper 2003-6968, 2003.

[3] Nelson, H.F., and Riggins, D.W., "Hypersonic Flow Control Using Upstream Focused Energy Deposition," AIAA Journal, Vol. 38, No. 4, 2000, pp. 723-725.

[4] Riggins, D. R., Nelson, H. F., Johnson, E., "Blunt-Body Wave Drag Reduction Using Focused Energy Deposition," AIAA Journal, Vol. 37, No. 4, 1999, pp. 460-467.

[5] Bisek, N., Boyd, I., and Poggie, J., "Numerical Study of Plasma-Assisted Aerodynamic Control for Hypersonic Vehicles," Journal of Spacecraft and Rockets, Vol. 46, No. 3, May-June 2009, pp. 568-576.

[6] Menart, J., Stanfield, S., Shang, J., Kimmel, R., and Hayes, J., "Study of Plasma Electrode Arrangements for Optimal Lift in a Mach 5 Flow," AIAA Paper 2006-1172, January 2006.

[7] Shneider, M. N., Macheret, S. O., Zaidi, S. H., Girgis, I. G., and Miles, R. B., "Virtual Shapes in Supersonic Flow Control with Energy Addition," AIAA Journal of Propulsion and Power, Vol. 24, No. 5, September-October 2008, pp. 900-915.

[8] Guo, R., and Tan, H., "Experimental Study of the Unstable-Unstarted Condition of a Hypersonic Inlet at Mach 6," Journal of Propulsion and Power, Vol. 23, No. 4, July-August 2007, pp. 783-788.

[9] Heiser, W., and Pratt, D., Hypersonic Airbreathing Propulsion, AIAA Education Series, AIAA, 1994.

[10] Curran, E. T., and Murthy, S. N. B. (eds.), Scramjet Propulsion, Vol. 189, Progress in Astronautics and Aeronautics, AIAA, 2000.

[11] http://vulcan-cfd.larc.nasa.gov/, VULCAN Homepage, June 2009.

[12] Morrison, J.H., and White, J.A., "A Pseudo-Temporal Multi-Grid Relaxation Scheme for Solving the Parabolized Navier-Stokes Equations", AIAA Paper 99-3360, 1999.

[13] Rodriguez, C. G., "Asymmetric Effects in Numerical Simulation of Supersonic Flows with Upstream Separated Regions," AIAA Paper 2001-0084, 2001.

[14] Goyne, C.P., Krauss, R.H., McDaniel, J.C., and Rodriguez, C.G., "Experimental and Numerical Study of a Dual-Mode Scramjet Combustor", AIAA Paper 2002-5216, 2002.

[15] Cutler, A. D., and White, J. A., "An Experimental and CFD Study of a Supersonic Coaxial Jet," AIAA Paper 2001-0143, 2001.

[16] Rodriguez, C., Riggins, D., and White, J., "Three-Dimensional Effects in Modeling of Dual-Mode Scramjets," AIAA Paper 2000-3704, 2000.

[17] Menter, F., "Improved Two-Equation k-w Turbulence Models for Aerodynamic Flows," NASA TM 1103975, October 1992.

[18] Riggins, D., Tackett, R., Taylor, T., and Auslender, A. "Thermodynamic Analysis of Dual-Mode Scramjet Engine Operation and Performance," AIAA Paper 2006-8059, 2006.

[19] Anderson, J.D., Computational Fluid Dynamics, McGraw-Hill, Inc., 1995.

VITA

Matthew Flynn Rohweder was born in Moline, IL on November 28th, 1979. He graduated from Rock Island Alleman High School in May 1998 before enrolling in the University of Missouri-Rolla in August 1998. He graduated in May 2002 with his Bachelor of Science degree in Aerospace Engineering. After graduation, he completed the Navy's Officer Candidate School and received his commission as an Ensign in the United States Navy on September 6, 2002. After completing his training in naval nuclear propulsion, he served aboard the USS SAN FRANCISCO, SSN 711, from April 2004 through October 2006 where he qualified Submarine Warfare and was certified as a Nuclear Engineering Officer. He then volunteered and served ten months with the Army's 3rd Brigade Combat Team, 25th Infantry Division in Kirkuk, Iraq from December 2006 through October 2007 as an Electronic Warfare Officer before leaving active duty service. He completed his Master of Science degree in Aerospace Engineering from the Missouri University of Science and Technology (formerly University of Missouri-Rolla) in May, 2010.